Heliyon 5 (2019) e02154

Contents lists available at ScienceDirect

Heliyon

www.elsevier.com/locate/heliyon

Robust fractional-order auto-tuning for highly-coupled MIMO systems

Jasper Juchem [a,b,*], Cristina Muresan [c], Robain De Keyser [a,b], Clara-Mihaela Ionescu [a,b,c]

[a] Department of Electrical Energy, Metals, Mechanical Constructions and Systems, Ghent University, Technologiepark 125, 9052 Zwijnaarde, Belgium
[b] EEDT core lab on decision and control, Flanders Make Consortium, Technologiepark 131, 9052 Zwijnaarde, Belgium
[c] Department of Automation, Technical University of Cluj–Napoca, Str. G. Baritiu nr. 26–28, 400027 Cluj–Napoca, Romania

ARTICLE INFO

Keywords:
Systems engineering
Systems theory
Control systems
Control system design
Automation
Computer-aided engineering
Robustness analysis
Fractional-order control
Office lighting
Fractional control implementation
Auto-tuning
Highly-coupled systems

ABSTRACT

Many processes in industry are highly-coupled Multiple-Input Multiple-Output (MIMO) systems. In this paper, a methodology, based on the *Kissing Circle* (KC) tuning method, is proposed to tune a fractional-order PI controller for these types of systems. The KC method relies on frequency domain specifications and emphasizes improving robustness. The method does not require a model, a single sine test suffices to obtain the controller parameters. Hence, the method can be categorized as an auto-tuner. For comparison, an integer-order PI is tuned with the same requirements. To evaluate and analyze the performance of both controllers an experimental test bench is used, i.e. a landscape office lighting system. A direct low-order discretization method is used to implement the controller in a real process. Both controllers are subjected to simulation experiments to test the performance in time and frequency domain and they are subjected to process variations to evaluate their robustness. The fractional controller manages to control a process that is susceptible to 85% variation in time constant mismatch as opposed to 79% for the integer-order controller. An Integer Absolute Error evaluation of experimental results show that the fractional-order PI controller and integer-order PI controller have similar control performance, as expected from the frequency domain analysis. As model uncertainty can add up in MIMO systems, improved robustness is crucial and with this methodology the control performance does not deteriorate. Moreover, a decrease in power consumption of 6% is observed.

1. Introduction

The transition wave of Industry 4.0 has pushed companies to improve the automation capabilities of their plants. Previously, the focus was put on control and automation of a single manufacturing step in a production process. Nowadays, the target is to shift more and more towards the holistic approach of plant-wide control [1, 2, 3]. Consequently, systems that need automation are expanding, which includes that subsystem interaction becomes increasingly important in the technological landscape [4]. In this context, robustness, flexibility, and user-specificity become very relevant [5].

A recent survey on the relevance of control strategies in industry has shown that PID (Proportional-integral-derivative) control and MPC (Model predictive control) are maintaining the position at the top of the charts [6]. PID still has the upper hand, because of its simplicity and effectiveness in a manifold of cases. However, PID lacks performance in complex situations. First of all, PID has a single input and a single output, thus, it is often being used in a decentralized context. In [7], it is shown that for large-scale applications a decentralized architecture would only be acceptable if weak coupling exists between the subsystems. This would limit its applicability dramatically. Secondly, the controller has a limited amount of tuning parameters. In terms of simplicity, this can be a strength. However, it reduces the flexibility to approve with certain tuning rules. Therefore, the controller can only fulfill a limited number of conditions, often leading to suboptimal control. Thirdly, PID cannot handle sinusoidal disturbances [8] and constrained processes without extensive adaptations to the control strategy [9]. The MPC controller does not suffer from the above and it has been proven in [5] and [1] that it can handle MIMO systems with significant coupling. However, it comes with a price: the design and implementation of the controller is a task that demands sufficient insight in and knowledge of the controller and the process. Therefore, industry is hesitant to implement advanced control strategies.

Lately, fractional calculus has attracted the interest of engineers and applied scientists [10, 11, 12]. In [13], it is argued that the adoption of fractional calculus in control stimulates new opportunities. Fractional-

* Corresponding author at: Department of Electrical Energy, Metals, Mechanical Constructions and Systems, Ghent University, Technologiepark 125, 9052 Zwijnaarde, Belgium.
E-mail address: Jasper.Juchem@UGent.be (J. Juchem).

https://doi.org/10.1016/j.heliyon.2019.e02154
Received 24 April 2019; Received in revised form 3 July 2019; Accepted 22 July 2019

calculus, resorting under the branch of mathematical analysis, is a matter of differentiation and integration of non-integer orders, which is in a matter of fact a generalization of the latter. It is purely a matter of the control engineer's own convenience to use these new controllers for complex natural or man-made systems. The extra parameters generate extra degrees of freedom (DOF), which in return provides more precise tuning of the closed-loop process [14, 15]. Recently, tuning of fractional-order $PI^{\lambda}D^{\mu}$ controllers has attracted the interest of several researchers, because of its enhanced control quality and its simplicity [16, 17]. In [18], the author presents a new auto-tuning method called the *Kissing Circle* (KC) method, which is later adapted for tuning of fractional-order PID controllers [19]. In the method, certain frequency domain specifications, i.e. gain cross-over frequency, phase margin, and the iso-damping property, are imposed on the open-loop process. Several examples exist of theoretical and experimental implementations on Single-Input Single-Output (SISO) systems of this method [20, 21, 22].

In this paper, it is proven that the KC method can be used to tune a fractional-order PI (FOPI) controller for highly-coupled, integer-order, MIMO systems, as opposed to [23], where an integer-order controller is used to control a fractional-order MIMO system. For these types of systems a robust controller is needed, because it is difficult to obtain a high identification accuracy. The KC method tunes the controller based on robustness specifications. Therefore, it is reasonable to assume that the FOPI, would improve the control performance of a highly-coupled MIMO system. For comparison, an integer-order PI controller is tuned under similar conditions. The tuning strategy is done for an office lighting test bench. As office lighting is responsible for a significant amount of the energy consumption in commercial buildings and lighting quality has a significant effect on the performance of the employees, proper control is inevitable [24]. The goal is to achieve optimal light intensity on eight desks, using eight lamps. The lamp's electrical power input is the manipulated variable. This motivated the research in [25] to tune a PID controller for lights as a minimization of electrical power consumption. Each lamp, and by expansion any light source, will influence the light intensity on each desk. The theoretical robustness to time constant variations of both controllers is researched. In an experiment, the ability of handling disturbance, uncertainty, and reference-tracking is checked.

This paper is structured as follows: the next section addresses the tuning of both the integer-order and fractional-order PI. The test bench is discussed and some remarks are made on the implementation of the controller. The third section presents the simulation and experimental results of both controllers on the test bench. Conclusions are formulated in section five.

2. Method

Tuning of $PI^{\lambda}D^{\mu}$ can be done in various ways: based on optimization techniques [25, 26], Ziegler-Nichols rules [27, 28], frequency domain specifications [29, 30, 22] and many more [31, 32]. In [32] an attempt is made to compare different tuning rules, but this is a very limited study. Most of these techniques rely on process model. In MIMO systems obtaining an accurate process model leads to significant errors due to the subsystem interaction. Therefore, model-free tuning is preferred in this context. Auto-tuners for FOPID are rare [33]. Moreover, robustness to process variation is a key parameter in the context of MIMO control. The frequency domain based techniques specifically rely on robustness measures. In [22], a auto-tuner based on frequency domain specifications is proposed for SISO systems. This *Kissing Circle* (KC) method fulfills all aforementioned requirements to be suitable for a MIMO setup with high interaction. Moreover, in [34] it is stated that the method overcomes pitfalls present in other (automatic) tuning methods. The aforementioned literature motivate the choice for this auto-tuning method in this case.

In this section, the design of a fractional-order PI (FOPI) controller with the KC method is discussed. Some frequency domain specifications are used to find the appropriate parameters of the controller. For comparison, an integer-order PI (IOPI) controller is tuned under similar conditions.

2.1. Fractional-order PI

The fractional-order PI has the following transfer function:

$$C(s) = k_p\left(1 + \frac{k_i}{s^{\lambda}}\right) \tag{1}$$

with $k_p, k_i \in \mathbb{R}_{\geq 0}$ the proportional and the integral gain respectively, and $\lambda \in (0, 2]$ the fractional order. The FOPI is a generalization of the IOPI as for the latter, λ is limited to integer numbers, i.e. one.

The FOPI controller has three unknowns: k_p, k_i, and λ. To determine the values of the three unknowns, it is needed to define a set of three performance specifications that need to be fulfilled. In [22] a strategy is described to tune a FOPI with frequency domain specifications. The technique is classified as an auto-tuning method, which is a powerful tool in industry, as it is beneficial to avoid spending costly time on tuning low-hierarchical controllers. Nevertheless, few Fractional Order Control (FOC) strategies with auto-tuning have been proposed [33]. A few examples are the phase shaper as presented in [35], the method based on a relay test in [36], and an auto-tuner based on the Ziegler-Nichols tuning procedure in [37].

In this case, the fractional-order KC method will be used to tune the controller [19]. The following properties will be used to determine the controller parameters [38]:

1. Gain cross-over frequency ω_{gc}: this parameter is directly proportional to the settling time of the closed-loop system. The gain cross-over frequency is the frequency for which the magnitude of the open-loop transfer function becomes one. This leads to the first performance equation:

   $$|H_{OL}(j\omega_{gc})| = 1 \tag{2}$$

   Here, $H_{OL}(s) = C(s) \cdot R(s)$ refers to the open-loop transfer function [39]. Here, $\omega_{gc} = 75$ rad/s is chosen as a trade-off between bandwidth and robustness. It is advisable to select the gain cross-over frequency close to the break frequency of the process.
2. Phase margin ϕ_m: this is an indicator of the system's stability. The phase margin (PM) is defined as the phase difference with $-\pi$ at the gain cross-over frequency [39]. This means that if the PM approaches 0°, which is defined at the frequency where the magnitude of the open-loop transfer function is equal to one, the closed-loop transfer function approaches instability, i.e. the transfer function's denominator approaches zero. The second criterion is defined as follows:

   $$\angle H_{OL}(j\omega_{gc}) = -\pi + \phi_m \tag{3}$$

   The PM $\phi_m = 60°$ is chosen.
3. Iso-damping property: this property realizes increased robustness to process model changes. Also, the overshoot is approximately held constant within a gain range. The constant overshoot is achieved by maintaining a constant phase margin around the gain cross-over frequency. This can be simplified to the condition that the phase should be constant around the frequency ω_{gc} [38]. The iso-damping property is expressed in the following equation:

   $$\left.\frac{d(\angle H_{OL}(j\omega))}{d\omega}\right|_{\omega=\omega_{gc}} = 0 \tag{4}$$

The KC method splits the Nyquist plane up in two complementary regions: a forbidden and a permitted region. The forbidden region is the area that the open-loop transfer function must avoid. Here, the forbidden region is defined as a circle with radius R and center C. The

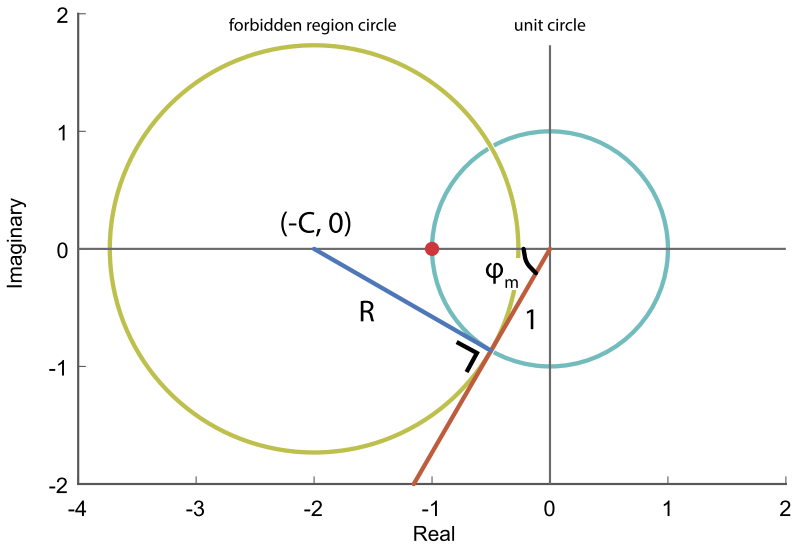

Fig. 1. Construction of the forbidden region in the Nyquist plane for the KC method.

forbidden region contains the unstable point $(-1,0)$. To determine the forbidden region center $-C \in \mathbb{R}^-$ and radius R, the aforementioned specifications are used. The PM should be respected, whereas keeping it as low as possible to achieve a faster rise time, such that the forbidden region circle touches the beeline specified by the angle ϕ_m with the real axis, and this on the location where the modulus of the open-loop transfer function becomes one, i.e. where the PM slope crosses the unity circle. To achieve the iso-damping property the open-loop transfer function should be tangent to the forbidden region circle. This results in the fact that the line perpendicular to the PM slope crosses the real axis in the point $-C$, which also fixes R. In Fig. 1 a visualization is given. Now, trigonometric relations can be used to calculate the radius and the center of the forbidden region:

$$C = \frac{1}{\cos(\phi_m)} \tag{5}$$

$$R = \sqrt{C^2 - 1} \tag{6}$$

Next, the slope of the forbidden region is calculated, as it will be the reference of the tangent line of the open-loop process transfer function for the gain cross-over frequency (iso-damping). This is the slope of the PM line through the origin:

$$\begin{aligned} S_{fr} &= \tan(\phi_m) \\ &= \sqrt{3} \end{aligned} \tag{7}$$

Then, the properties of the gain cross-over frequency and phase margin are used to determine the open-loop frequency response at ω_{gc}:

$$\begin{aligned} H_{OL}(j\omega_{gc}) &= M_{gc} e^{j\phi_{gc}} \\ &= \cos(-\pi + \phi_m) + j\sin(-\pi + \phi_m) \end{aligned} \tag{8}$$

because $M_{gc} = 1$ and $\phi_{gc} = 180° + \phi_m$ from equations (2) and (3) respectively. The open-loop transfer function is the succession of the controller $C(s)$ and the process $R(s)$ with the decoupling in place:

$$\begin{aligned} H_{OL}(s) &= C(s) \cdot R(s) \\ \Leftrightarrow C(j\omega_{gc}) &= \frac{H_{OL}(j\omega_{gc})}{R(j\omega_{gc})} \\ &= a + bj \end{aligned} \tag{9}$$

Using

$$\begin{aligned} j^\alpha &= \left(\exp\left(j\frac{\pi}{2}\right)\right)^\alpha \\ &= \exp\left(j\frac{\alpha\pi}{2}\right) \\ &= \cos\left(j\frac{\alpha\pi}{2}\right) + j\sin\left(j\frac{\alpha\pi}{2}\right) \end{aligned} \tag{10}$$

the controller can be expressed in frequency domain as follows:

$$C(j\omega) = k_p\left(1 + k_i\omega^{-\lambda}\left(\cos\frac{\lambda\pi}{2} - j\sin\frac{\lambda\pi}{2}\right)\right) \tag{11}$$

This leads to the following solution for the parameters $k_p, k_i = f(\lambda)$:

$$k_p = \frac{1}{x\sin\left(\frac{\lambda\pi}{2}\right)} \tag{12}$$

$$k_i = -\frac{b}{x\omega^{-\lambda}} \tag{13}$$

$$x = a\sin\left(\frac{\lambda\pi}{2}\right) + b\cos\left(\frac{\lambda\pi}{2}\right) \tag{14}$$

Finally, the optimal fractional parameter λ_{opt} needs to be found, such that the slope of the open-loop transfer function in ω_{gc} is equal to S_{fr}. The slope of the open-loop transfer function is found as follows:

$$\begin{aligned} \left.\frac{dH_{OL}(j\omega)}{d\omega}\right|_{\omega=\omega_{gc}} &= \left.\frac{dC(j\omega)}{d\omega}\right|_{\omega=\omega_{gc}} R(j\omega_{gc}) + C(j\omega_{gc})\left.\frac{dR(j\omega)}{d\omega}\right|_{\omega=\omega_{gc}} \\ &= \left.\frac{dRe_H}{d\omega}\right|_{\omega=\omega_{gc}} + j\left.\frac{dIm_H}{d\omega}\right|_{\omega=\omega_{gc}} \end{aligned} \tag{15}$$

The slope in the Nyquist plane is given by

$$\begin{aligned} S_H &= \left.\frac{dIm_H}{dRe_H}\right|_{\omega=\omega_{gc}} \\ &= \left.\frac{dIm_H}{d\omega}\right|_{\omega=\omega_{gc}} \Big/ \left.\frac{dRe_H}{d\omega}\right|_{\omega=\omega_{gc}} \end{aligned} \tag{16}$$

The function $||S_{fr} - S_H(\lambda)||$ needs to be minimized with $\lambda \in [\lambda_{min}, 2]$. Originally, λ was assumed to be ranging from zero to two, but this does not guarantee a physical meaning of the controller parameters, i.e. positive constants k_p and k_i [40].

2.2. Integer-order PI

The integer-order PI controller has the following form:

$$C(s) = k_p\left(1 + \frac{k_i}{s}\right) \tag{17}$$

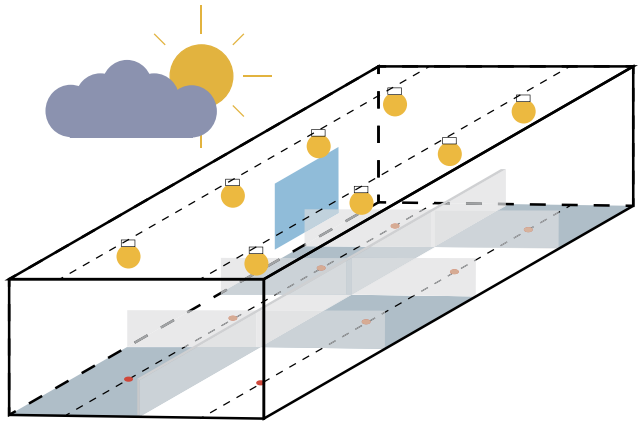

Fig. 2. Schematic representation of the light setup. The box contains eight zones that are separated by walls with a height that is smaller than the height of the box. Each zone has a lamp and a light sensor.

To be able to make a fair comparison with FOPI, the same performance parameters and values are used as in the previous tuning rules. An important difference between the IOPI and the FOPI is that the former has two DOF as compared to three for the latter. Therefore, it is necessary to eliminate one of the conditions given by equations (2), (3) and (4). It is difficult to achieve condition (4) without fulfilling condition (2) and (3). Therefore, the iso-damping condition is removed. The gain cross-over frequency $\omega_{gc} = 75$ rad/s and the phase margin $\phi_m = 60°$ are chosen similar to the FOPI design parameters.

The correlation between the open-loop process and the controller in the gain cross-over frequency is given by equation (9). This can be combined with the equation of an IOPI controller (17) evaluated at the gain cross-over frequency $s = j\omega_{gc}$, which leads to the following set of formulas for the controller parameters:

$$k_p = a \tag{18}$$

$$k_i = \frac{-b\omega_{gc}}{a} \tag{19}$$

2.3. Test bench: office lighting

The test bench consists of a box that is subdivided into eight zones which are separated by small walls (see Fig. 2). Every zone has a lamp (*incandescent light bulb, CML 1847*) and a light sensor (*LDR, 1kΩ*). The steering of the lamps and the reading of the sensors is done with dSPACE™ DS1104 R&D Controller Board. Between the different zones there exists high coupling as the light of a lamp disperses omni-directional. The system is subjected to certain constraints, i.e. the input voltage to a lamp is limited to the range $[0, 5]$ V. The lower limit has a physical rationale: a lamp is unable to retract light from a room. As the same lamps and sensors are used in every zone, it can be assumed that the dynamics are similar for every zone. Remember that the influence of a lamp on a certain sensor is inversely correlated to the distance between these two objects. Therefore, the process is modeled as a single transfer function, representing the dynamics, multiplied by an eight-by-eight gain matrix [8]. The process dynamics are given by the transfer function:

$$P(s) = \frac{3666.6}{s^2 + 124.1s + 3726} \tag{20}$$

with s the Laplace variable.

The gain matrix is given in equation (21).

$$\mathbf{C} = \begin{bmatrix} 1.00 & 0.67 & 0.34 & 0.23 & 0.61 & 0.47 & 0.31 & 0.23 \\ 0.70 & 0.80 & 0.62 & 0.39 & 0.53 & 0.54 & 0.44 & 0.32 \\ 0.56 & 0.59 & 0.81 & 0.66 & 0.32 & 0.41 & 0.58 & 0.34 \\ 0.19 & 0.27 & 0.56 & 1.05 & 0.23 & 0.26 & 0.46 & 0.73 \\ 0.57 & 0.41 & 0.26 & 0.20 & 0.98 & 0.67 & 0.33 & 0.22 \\ 0.49 & 0.40 & 0.39 & 0.30 & 0.63 & 0.83 & 0.61 & 0.36 \\ 0.30 & 0.44 & 0.56 & 0.50 & 0.41 & 0.64 & 0.83 & 0.59 \\ 0.21 & 0.23 & 0.44 & 0.66 & 0.24 & 0.31 & 0.60 & 0.97 \end{bmatrix} = (c_{ij}) \tag{21}$$

Here, the row number i refers to the lamp and the column number j refers to the sensor. The senors and lamps introduce some non-linearities [8]. For convenience, these are linearized in the middle of the input range. This leads to an additional gain $G = 0.42$. The entire system's model is given by equation (22).

$$\mathbf{Q}(s) = G \cdot P(s) \cdot \mathbf{C} \tag{22}$$

2.3.1. Static decoupler

In this section, the design of a decoupler for the MIMO system is discussed. This means that the input signal to the process is conditioned in such a way that the coupling effect is counteracted. The static decoupler is based on the steady state of the process, i.e. $\mathbf{Q}_0 = \mathbf{Q}(0)$. The rationale behind the concept of static decoupling is the following:

$$\mathbf{D}\mathbf{Q}_0 = \boldsymbol{I}_8 \tag{23}$$

Here, $\mathbf{D} \in \mathbb{R}^{8\times8}$ is the decoupler matrix, i.e. the conditioning matrix of the process input, and $\boldsymbol{I}_8$ is an identity matrix of size eight. From equation (23) it follows that

$$\mathbf{D} = \boldsymbol{I}_8 \mathbf{Q}_0^{-1} \tag{24}$$

This is possible as $\mathbf{Q}_0$ is invertible. The decoupled process has the following model

$$\mathbf{T}(s) = \frac{P(s)}{P(0)} \cdot \mathbf{D}\mathbf{Q}_0 = \frac{3667}{0.984s^2 + 122.1s + 3667} \boldsymbol{I}_8 \tag{25}$$

Notice that in (25) the coupling effects are now eliminated as all off-diagonal elements are zero. Every output is linked to only one single input.

2.3.2. Implementation of the controllers

The frequency response and the slope of the phase of the process $R(j\omega)$ for the selected gain cross-over frequency ω_{gc} can be found from a single sine test. In [22], a method is discussed to find the aforementioned parameters without the need for a model. A sine signal $u(t)$ with a frequency ω_{gc} and amplitude 1 is applied to the decoupled process. The output of the process is compared with the input to find the magnitude and the phase for the gain cross-over frequency. To find the slope the process output is filtered with the transfer function

$$F(s) = \frac{2s}{s^2 + \omega_{gc}^2} \tag{26}$$

This leads to the time signal $x(t)$. Next, a time series is obtained by the following operations $\bar{y}(t) = x(t) - t \cdot y(t)$. The three time series $u(t)$, $y(t)$, and $\bar{y}(t)$ are given in Fig. 3. The phase slope at the gain cross-over frequency can be found from

$$\frac{d\phi}{d\omega}|_{\omega=\omega_{gc}} = \frac{\bar{M}}{M} cos(\bar{\phi} - \phi) \tag{27}$$

with $\bar{M}$, $\bar{\phi}$, M, and ϕ the modulus and phase of $\bar{y}(t)$ and $y(t)$ respectively. From the data vectors presented in Fig. 3 the following numerical values are derived.

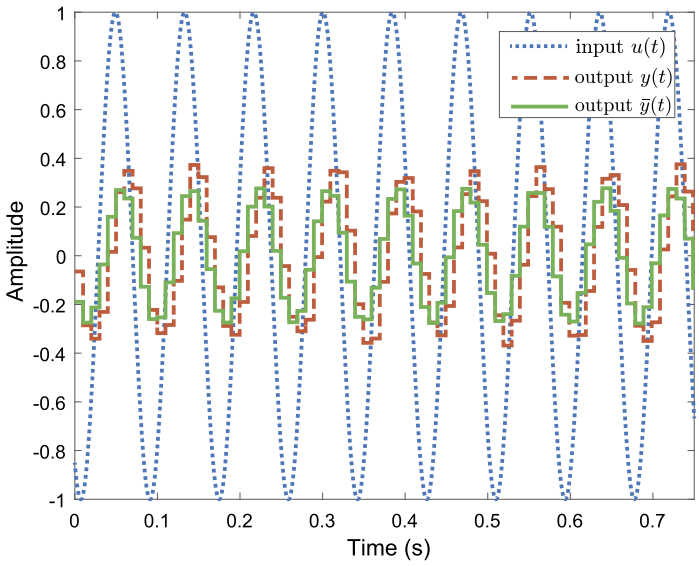

Fig. 3. The results of the sine test at ω_{gc}: the input signal $u(t)$, the process output $y(t)$, and the signal $\bar{y}(t)$ to find the phase slope.

Table 1
Integer-order and Fractional-order PI parameters for the continuous time transfer function.

Type	k_p	k_i	λ
IOPI	1.45	103.09	–
FOPI	1.22	89.96	0.927

$$R(j\omega_{gc}) = 0.12 - 0.33j$$

$$\frac{d\angle R(j\omega)}{d\omega}|_{\omega=\omega_{gc}} = -21°$$

In this case, the model of the test bench is known from [8]. This means that the single sine test (see Fig. 3) and its numerical results can be validated. With the decoupler in place, the process transfer function is given by (25). A first-order approximation is used. This is justified by the processes' transient of the step response. The approximated transfer function is given by

$$R(s) = \frac{1}{0.036s + 1} \tag{28}$$

Using the model the following parameters are obtained:

$$R(j\omega_{gc}) = 0.1206 - 0.3257j$$

$$\frac{d\angle R(j\omega)}{d\omega}|_{\omega=\omega_{gc}} = -15°$$

These numerical results seem to confirm the results obtained with the sine test, they have a similar order of magnitude. This confirms that the sine test gives a decent result and can be used to obtain the parameters that are required for the KC method.

To obtain the fractional-order PI, equation (9) needs to be evaluated, which leads to the solution:

$$a = 1.45$$

$$b = -1.99$$

Based on these values the IOPI and FOPI parameters k_p, k_i, and λ are evaluated. The results are given in Table 1.

The controllers need to be transformed to their discretized form as they will be implemented on a digital system. For the FOPI, the frequency response is approximated with a low-order direct discrete-time implementation. In [41] an efficient algorithm is presented. The method is based on the impulse response. An interpolation of the Euler and Tustin discretization is used:

$$\hat{s}(q) = \frac{1+\alpha}{T_s}\frac{1-q}{1+\alpha q} \tag{29}$$

In this equation $q = z^{-1}$, z is the z-transform variable, $T_s = 0.01$ s is the sampling time, and $\alpha \in [0, 1]$ the interpolation parameter. If $\alpha = 0$, $\hat{s}(q)$ is the Euler discretization rule. In the other extreme, if $\alpha = 1$, equation (29) is the Tustin discretization. This parameter has a weighting effect on the frequency response, establishing a trade-off between penalizing the error on the magnitude or the phase. Here, α is set to 0.9. The order of the rational discrete transfer function is chosen to be $N = 4$. This is again a trade-off design parameter. A high N guarantees a better accuracy of the approximation, as a lower N decreases complexity of the transfer function, i.e. less poles and zeros. The discretized approximation is given in Table 2. For the discretization of the IOPI, the Tustin method is used, as this method gives good results for integer order systems:

$$\hat{s}(q) = \frac{2}{T_s}\frac{1-q}{1+q} \tag{30}$$

with $q = z^{-1}$, z is the z-transform variable, $T_s = 0.01$ s is the sampling time. The resulting transfer function is given in Table 2.

Table 2
The discretized Integer-order and Fractional-order PI controller.

Type	Discrete transfer function $\boldsymbol{C(q)}$
IOPI	$\frac{2.19q^{-1}-0.70}{q^{-1}-1}$
FOPI	$\frac{1.86q^4-5.92q^3+6.76q^2-3.19q+0.49}{q^4-3.85q^3+5.55q^2-3.55q+0.85}$

The coefficients of the transfer functions are rounded. Rounding can lead to erroneous, i.e. unstable, results. Therefore, it is important to save a sufficient amount of decimal numbers for the actual implementation.

3. Results

In this section, the performance of both controllers on the test bench are compared from a theoretical and experimental point of view. First, the robustness to time constant variation is evaluated in simulation. Secondly, the controllers' performance is checked. An experiment will

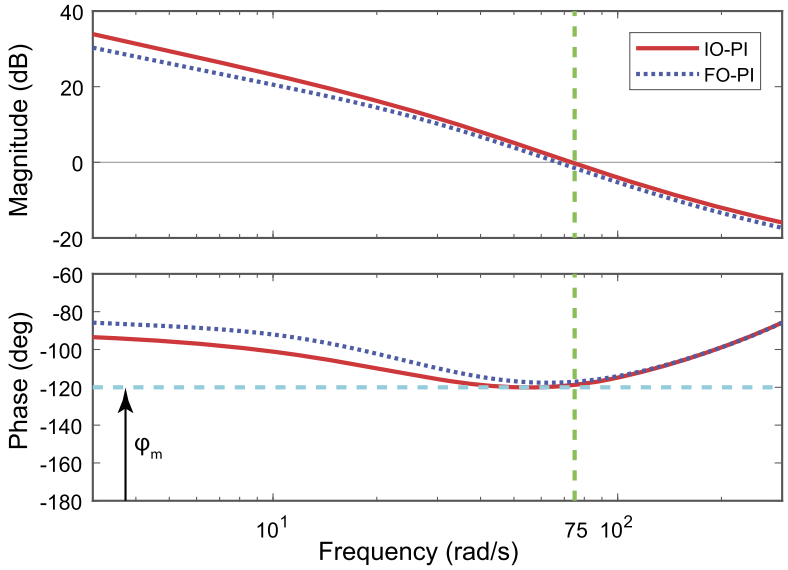

Fig. 4. The Bode plot shows the (*top*) magnitude and (*bottom*) phase of the open-loop system $H_{OL}(s)$ with the discretized IOPI and FOPI controller.

show the effect of the static decoupler and the controllers performance for zero-error tracking. For comparative reasons, the same experiment will be run for the IOPI and the FOPI controller as designed in section 3.

3.1. Simulation analysis

In this section, a theoretical analysis is done for the integer- and fractional-order controller with regard to frequency domain specifications and robustness to time constant variation.

To compare both controllers, a graphical analysis in frequency and time domain is performed. First, the Bode plots in Fig. 4 are inspected. This shows that it is possible to achieve particular design specifications due to the fractional integrator. The IOPI controller is able to fulfill the specifications at the gain cross-over frequency, but close to that frequency the phase tends to drop below the $-120°$ line, which affects the stability slightly. From the Bode plot, one can discern the integer-order from the fractional-order open-loop transfer function: the phase for integer-order integrator is $-90°$ at low frequencies and the slope of the magnitude is -20 dB/dec, while for the fractional-order case the phase is $-90° \cdot \lambda$ and the slope of the magnitude is $-20 \cdot \alpha$ dB/dec [38, 42].

Secondly, to show the effect of the iso-damping property, the Nyquist plot is checked. In Fig. 5, three open-loop transfer functions are plotted. The FOPI controller's ability to handle a $+/-30\%$ process gain error is shown without violating the PM and gain cross-over requirement. As the gain changes the open-loop transfer function tends to roll against the edge of the circle, without entering the forbidden region. This results in a low variation on the damping and, thus, the overshoot. Also, the stability stays unchanged for gain variations. From this, one can conclude that the controller is robust, as specified by the design specifications.

One could argue that the difference between the IOPI and FOPI case is negligible while observing the frequency domain plots 4 and 5. Also, the robustness, seems to be improved only marginally. Therefore, a third situation is simulated. In Fig. 6, the step response for uncertainty in the process' time constant τ is simulated, which is also linked to gain variation during the transient regime of the step response.

In Fig. 7, the pole of the closed-loop process with the FOPI controller is plotted in a pole-zero map for the same process' time constant variations as in Fig. 6. In the nominal case, this pole is located on the opposite side, as it has a positive real part. The complex pole pair for the nominal case, that is causing the oscillations in Fig. 8, shifts towards the imaginary axis, until it becomes a real number for increasing time

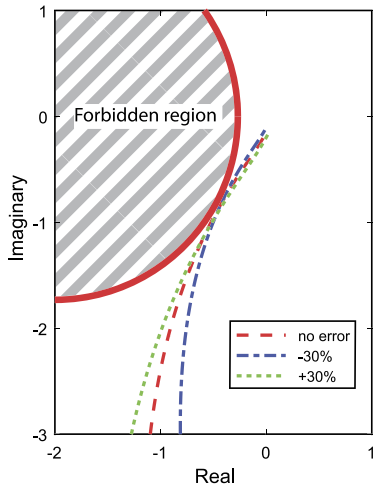

Fig. 5. The Nyquist plot of the open-loop system $H_{OL}(s)$ with the discretized FOPI controller and variations in the process gain.

constant variation. There, it is almost not affected by a further decrease of the process' time constant. It can be noticed that a pole of the nominal case is drifting towards the left. For the case of -85% the pole has almost left the stable area of the real-imaginary space. A further decrease of the time constant will lead to unstable behavior of the system. From Fig. 6, it is clear that these poles shift much faster outside the stable region for the IOPI case. Up and above -80% the pole has entered the unstable region.

However, in Fig. 6 the control effort of the step response for the FOPI controller case would have a pronounced decaying ripple for the pole placement given in Fig. 7. Consider the z-transform of a system with a real pole at $z = a$. After making a fractional expansion of the transfer function, a term of the form

$$\frac{bz}{z-a} \tag{31}$$

is obtained. The z-transform has the generating sequence

$$ba^k \qquad \text{for} \quad k = 0, 1, 2, \ldots \tag{32}$$

in its response. Based on the location of the pole, the response will differ. In the case that $0 \leq a < 1$, the response results in a sequence of positive, monotonically decreasing numbers. In the other case, when

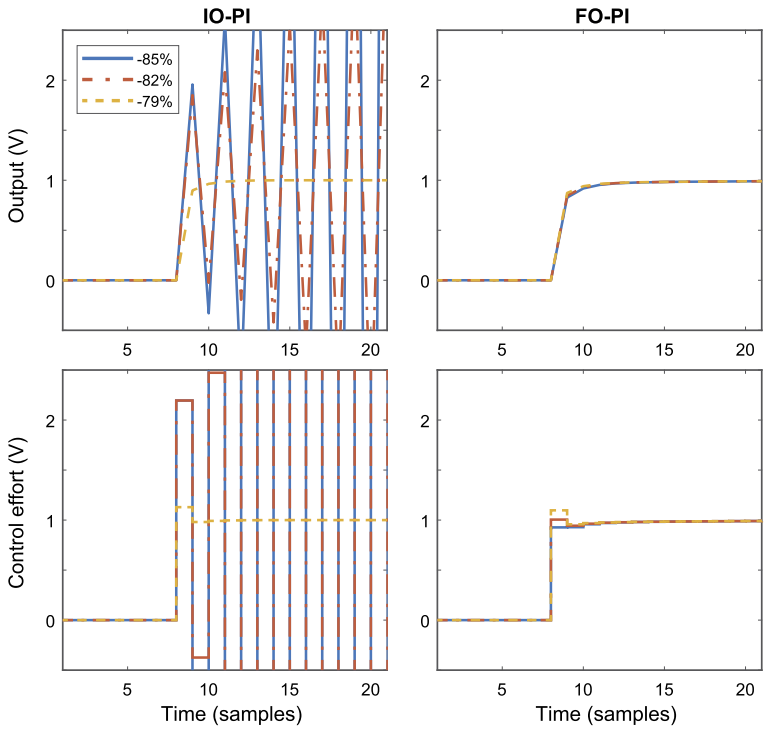

Fig. 6. The step response (*up*) and the control effort (*down*) are given for the closed-loop system for the IOPI (*left*) and FOPI (*right*) case.

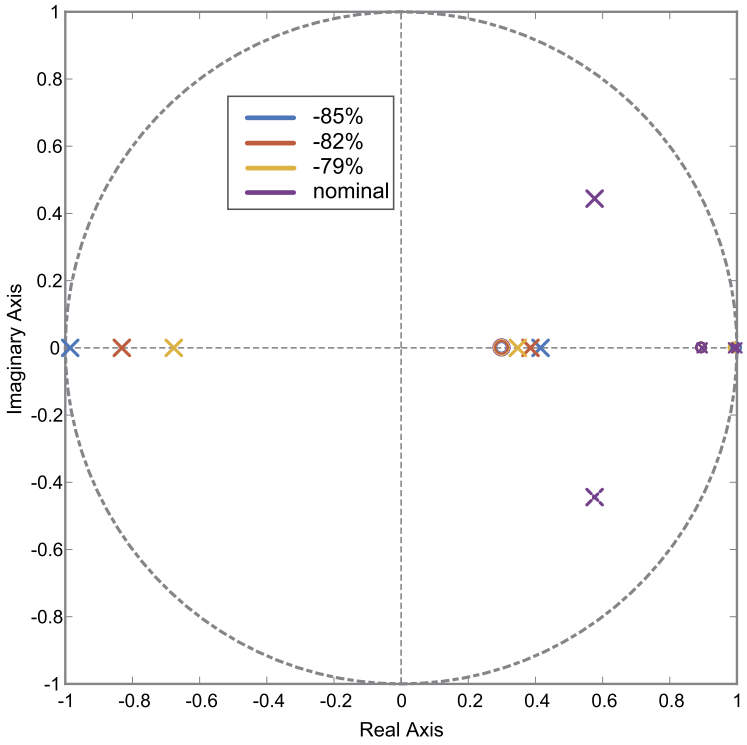

Fig. 7. The pole-zero map of the closed-loop system with the FOPI controller for process time constant variation.

$-1 < a \leq 0$, the response is a sequence of decaying numbers alternating in sign. This can introduce a ripple on the total system's response. The more the poles are located near the edge of the unit circle, the more dominant the poles will be in the total response. To remove this unwanted behavior a filter $F(z)$ is designed. The filter acts on the reference signal resulting in the closed-loop transfer function

$$\frac{F(z)R(z)C(z)}{1 + R(z)C(z)} \tag{33}$$

The filter will consist of a zero at the exact location of the closed-loop pole with a negative real part that does not leave the stable region of the z-domain, i.e. the unit circle. However, this is an improper transfer function. By adding a fast low-pass filter to the system the function is made proper, without influencing the response of the filtered transfer function. The filter needs to have a steady-state value of one, so all terms are normalized. The filter is given in the following

$$F(z) = \frac{z - p_u}{1 - p_u} \frac{1 - \epsilon}{z - \epsilon} \tag{34}$$

The first part of the filter is to cancel the unwanted pole p_u and the second part is the fast-acting low-pass filter with $\epsilon = 10^{-2}$. The filter is applied to both the IOPI and FOPI case, and the step response is given in Fig. 6. This figure shows that the IOPI controller has a harder time to keep the process stable under varying conditions, whereas the FOPI keeps the process stable up until 85% error on the time constant.

These simulation results indicate that the extra design effort for the FOPI can be worthwhile in terms of robustness. The increased design flexibility due to its extra DOF has led to superior control quality.

3.2. Experimental validation

In this section, the total light setup is observed. An experiment is designed which consists of two reference steps: one at zone 1 after 30 s from 2 V to 2.1 V, the other in zone 5 after 60 s from 2 V to 2.15 V. In the other zones a constant light intensity is demanded. Zones 2 and 3 are kept at 1.95 V, zones 4 and 6 at 2 V, zone 7 at 1.9 V, and zone 8 at 1.8 V. For the sake of simplicity, only zone 1 has been plotted in Fig. 8. To evaluate the overall quality of the controller, some indexes will be used. To evaluate the controllers ability to handle step changes and reject disturbances. This is done using the Integral Absolute Error (IAE) given by the following definition:

$$S_e = \sum_{i=1}^{8} \int_0^{\infty} |r_i(t) - y_i(t)| dt \tag{35}$$

The IAE of each zone is summed to give the final index.

In a system, the power consumption during the transient phase is equally relevant. As the electrical power is given by $P_{el}(t) = u(t)i(t)$ with $u(t)$ the voltage to a lamp (the control effort) and $i(t)$ the current running through the lamp. Due to Ohm's law, $P_{el}(t) = u(t)^2/R$. The resistance of the lamp is inherent to the design and is said to be constant. Consequently, the overall power consumption can be monitored by:

$$S_u = \sum_{i=1}^{8} \int_0^{\infty} u(t)^2 dt \tag{36}$$

In Table 3, the indexes are given for both controllers. These results confirm the assumption that in the nominal case very similar outputs are achieved for both controllers. The Bode plots in Fig. 4 are very similar. However, regarding energy consumption an improvement of 6% is observed. The FOPI controller can achieve a similar result using less electrical input power.

Table 3
The performance indexes IAE (S_e) and power consumption (S_u) for both controllers.

Type	S_e	S_u
IOPI	0.215	210.91
FOPI	0.215	197.83

From Fig. 8, the IOPI controller shows to have a higher overshoot (10%), but a little smaller settling time (5%), which agrees with the frequency response analysis. The control effort shows similar behaviour when it comes to the overshoot, the IOPI has a much higher peak with regard to the voltage over the lamp. The FOPI controller's output settles almost equally fast as the IOPI (3% slower), which results into less power consumption. The integrator assures zero tracking error in both cases. The coupling effect is almost completely canceled by the decoupler. This can be seen from the fact that in zone 1 there is almost no fluctuation as the step in zone 5 occurs. The zones that are closest to the stepped area show some fluctuations in the transient region, which can be expected as a static decoupler was designed for these experiments. In every zone, the controller is able to reject the step disturbance of the other zones. The further away from the zone, the less active the controller needs to be to compensate the disturbance.

4. Conclusions

In this paper, an auto-tuning methodology to design a fractional-order PI controller for a highly coupled MIMO system is discussed. Based on decoupler theory and the KC tuning algorithm the control strategy is obtained. To validate this methodology, a highly-coupled MIMO system is used: several lamps in a box need to be controlled to obtain a specified light intensity. To evaluate the controller's performance an integer-order PI controller is tuned as well, with similar conditions, to compare them. The results indicate that time constant variation is handled much better by the fractional-order controller: the fractional-order PI is able to maintain stability up until 85% variation as compared to the 79% variation for the integer-order PI. However, in the nominal case, a 10% smaller overshoot is observed. Nevertheless, the Integral Absolute Error (IAE) shows that both controllers perform equally well. Hence, we conclude that it is worthwhile to implement a fractional-order PI controller for highly-coupled MIMO systems, as the system's performance is maintained, while providing better robustness. Additionally, the fractional-order controller reduces the electrical power input with 6%, which is significant.

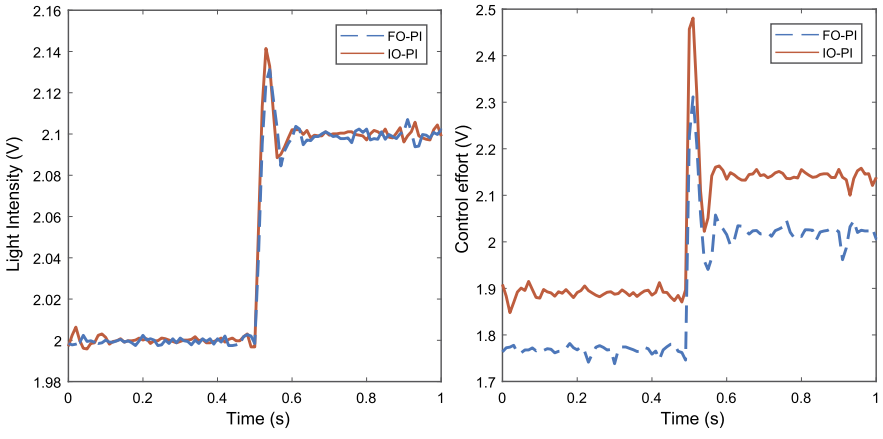

(a) (b)

Fig. 8. Detail of the step response in zone 1. (A) the output and (B) the control effort signals around the step for the IOPI and FOPI case.

Declarations

Author contribution statement

Jasper Juchem: Conceived and designed the experiments; Performed the experiments; Analyzed and interpreted the data; Contributed reagents, materials, analysis tools or data; Wrote the paper. Cristina Muresan: Conceived and designed the experiments; Analyzed and interpreted the data; Contributed reagents, materials, analysis tools or data; Wrote the paper. Robin De Keyser: Analyzed and interpreted the data; Contributed reagents, materials, analysis tools or data; Wrote the paper. Clara Mihaela Ionescu: Analyzed and interpreted the data; Wrote the paper.

Funding statement

Jasper Juchem and Clara M. Ionescu were supported by the Special Research Fund of Ghent University [STG020-18 MIMOPREC]. Cristina I. Muresan was supported by the Romanian National Authority for Scientific Research and Innovation [CNCS/CCCDI-UEFISCDI, project number PN-III-P1-1.1-TE-2016-1396, TE 65/2018].

Competing interest statement

The authors declare no conflict of interest.

Additional information

No additional information is available for this paper.

References

[1] D. Fu, H.-T. Zhang, Y. Yu, C.-M. Ionescu, E.-H. Aghezzaf, R. De Keyser, A distributed model predictive control strategy for the bullwhip reducing inventory management policy, IEEE Trans. Ind. Inform. 15 (2) (2019) 932–941.
[2] Q.P. He, J. Wang, Statistical process monitoring as a big data analytics tool for smart manufacturing, J. Process Control 67 (2018) 35–43.
[3] A. Maxim, D. Copot, C. Copot, C.-M. Ionescu, The 5w's for control as part of industry 4.0: why, what, who, and when - a PID and MPC control perspective, Inventions 9 (1) (2019) 1–9.
[4] M. Bauer, A. Horch, L. Xie, M. Jelali, N. Thornhill, The current state of control loop performance monitoring - a survey of application in industry, J. Process Control 38 (2016) 1–10.
[5] A. Maxim, D. Copot, R. De Keyser, C.-M. Ionescu, An industrially relevant formulation of a distributed model predictive control algorithm based on minimal process information, J. Process Control 68 (2018) 240–253.
[6] T. Samad, A survey on industry impact and challenges thereof, IEEE Control Syst. Mag. 37 (1) (2017) 17–18.
[7] R. Hermans, A. Jokić, M. Lazar, A. Alessio, P. van den Bosch, I. Hiskens, A. Bemporad, Assessment of non-centralised model predictive control techniques for electrical power networks, Int. J. Control 85 (8) (2012) 1162–1177.
[8] J. Juchem, S. Lefebvre, T. Mac Thi, C.-M. Ionescu, An analysis of dynamic lighting control in landscape offices, IFAC-PapersOnLine 51 (4) (2018) 232–237.
[9] L. Rundqwist, Anti-reset windup for PID controllers, IFAC Proc. 23 (8) (1990) 453–458.
[10] M.D. Ortigueira, Fractional Calculus for Scientists and Engineers, Springer, Berlin, Germany, 2011.
[11] H.G. Sun, Y. Zhang, D. Baleanu, W. Chen, Y.Q. Chen, A new collection of real world applications of fractional calculus in science and engineering, Commun. Nonlinear Sci. Numer. Simul. 64 (2018) 213–231.
[12] V.V. Uchaikin, Fractional Derivatives for Physicists and Engineers: vol. II. Applications, Springer, Berlin, Germany, 2013.
[13] Y.-Q. Chen, C.-M. Ionescu, Special issue: applied fractional calculus in modelling, analysis and design of control systems, Int. J. Control 90 (6) (2017) 1155–1156.
[14] A. Chevalier, C. Francis, C. Copot, C.-M. Ionescu, R. De Keyser, Fractional-order PID design: towards transition from state-of-art to state-of-use, ISA Trans. 84 (2019) 178–186.
[15] R. De Keyser, C.-M. Ionescu, Minimal information based, simple identification method of fractional order systems for model-based control applications, in: 2017 11th Asian Control Conference (ASCC), 2017, pp. 1411–1416.
[16] K. Bettou, A. Charef, Control quality enhancement using fractional $PI^{\lambda}D^{\mu}$ controllers, Int. J. Syst. Sci. 40 (8) (2009) 875–888.
[17] L. Dorčák, M. Papajová, F. Dorčáková, L. Pivka, Design of the fractional-order $PI^{\lambda}D^{\mu}$ controllers based on the optimization with self-organizing migrating algorithm, Acta Montan. Slovaca 12 (4) (2007) 285–293.
[18] R. De Keyser, C.-M. Ionescu, C.I. Muresan, Comparative evaluation of a novel principle for PID autotuning, in: 2017 11th Asian Control Conference (ASCC), 2017, pp. 1164–1169.
[19] R. De Keyser, C.I. Muresan, C.-M. Ionescu, Autotuning of a robust fractional order PID controller, IFAC-PapersOnLine 51 (25) (2018) 466–471.
[20] C. Copot, C. Muresan, C.-M. Ionescu, S. Vanlanduit, R. De Keyser, Calibration of UR10 robot controller through simple auto-tuning approach, Robotics 7 (35) (2018) 1–20.
[21] C.I. Muresan, C. Copot, I. Birs, R. De Keyser, S. Vanlanduit, C.-M. Ionescu, Experimental validation of a novel auto-tuning method for a fractional order pi controller on a ur10 robot, Algorithms 11 (7) (2018) 95–107.
[22] R. De Keyser, C.I. Muresan, C.-M. Ionescu, A novel auto-tuning method for fractional order PI/PD controllers, ISA Trans. 62 (2016) 268–275.
[23] D. Xue, T. Li, An approach to design controllers for MIMO fractional-order plants based on parameter optimization algorithm, ISA Trans. 82 (2018) 145–152.
[24] D. Flikweert, Position paper on the smartness indicator for buildings and lighting, Tech. rep., Lighting Europe, [Online], https://www.lightingeurope.org/images/publications/position-papers/LightingEurope_-_Position_Paper_-_20171129_-_on_smartness_indicator.pdf, 2017.
[25] C. Copot, T.M. Thi, C.-M. Ionescu, PID based particle swarm optimization in offices light control, IFAC-PapersOnLine 51 (4) (2018) 382–387.
[26] A. Biswas, S. Das, A. Abraham, S. Dasgupta, Design of fractional-order $PI^{\lambda}D^{\mu}$ controllers with an improved differential evolution, Eng. Appl. Artif. Intell. 22 (2) (2009) 343–350.
[27] D. Valério, J.S. da Costa, Tuning of fractional PID controllers with ziegler-nichols-type rules, Signal Process. 86 (10) (2006) 2771–2784.
[28] D.V. Dev, K.S. Usha, Modified method of tuning for fractional PID controllers, in: Proceedings of International Conference on Power Signals Control and Computations, 2014, pp. 8–10.
[29] R. Duma, P. Dobra, M. Trusca, Embedded application of fractional order control, Electron. Lett. 48 (24) (2012) 1526–1528.
[30] T.N.L. Vu, M. Lee, Analytical design of fractional-order proportional-integral controllers for time-delay processes, ISA Trans. 52 (5) (2013) 583–591.
[31] C. Muñiz-Montero, L.V. García-Jiménez, L.A. Sánchez-Gaspariano, C. Sánchez-López, V.R. González-Díaz, E. Tlelo-Cuautle, New alternatives for analog implementation of fractional-order integrators, differentiators and pid controllers based on integer-order integrators, Nonlinear Dyn. 90 (1) (2017) 241–256.
[32] R. Ranganayakulu, G.U.B. Babu, A.S. Rao, D.S. Patle, A comparative study of fractional order $PI^{\lambda}/PI^{\lambda}D^{\mu}$ tuning rules for stable first order plus time delay processes, Resour.-Efficient Technol. 2 (2016) S136–S152.
[33] I. Birs, C. Muresan, I. Nascu, C.-M. Ionescu, A survey of recent advances in fractional order control for time delay systems, IEEE Access 7 (2019) 30951–30965.
[34] R. De Keyser, C.I. Muresan, C.-M. Ionescu, Universal direct tuner for loop control in industry, IEEE Access 7 (2019) 81308–81320.
[35] Y.Q. Chen, K.L. Moore, B.M. Vinagre, I. Podlubny, Robust PID controller autotuning with a phase shaper, in: Proceedings of the First IFAC Workshop on Fractional Differentiation and Its Applications, 2004, pp. 162–167.
[36] C.A. Monje, B.M. Vinagre, V. Feliu, Y.Q. Chen, Tuning and auto-tuning of fractional order controllers for industry applications, Control Eng. Pract. 16 (2008) 798–812.
[37] C. Yeroglu, C. Onat, N. Tan, A new tuning method for $PI^{\lambda}D^{\mu}$ controller, in: Proceedings of the International Conference on Electrical and Electronics Engineering, 2009, pp. 312–316.
[38] C.A. Monje, Y. Chen, B.M. Vinagre, D. Xue, V. Feliu, Fractional-order Systems and Controls: Fundamentals and Applications, Springer, London, UK, 2010.
[39] G. Ellis, Control System Design Guide: Using your Computer to Understand and Diagnose Feedback Controllers, 4th edition, Elsevier Science, Oxford, UK, 2012.
[40] C.I. Muresan, I.R. Birs, C.-M. Ionescu, R. De Keyser, Tuning of fractional order proportional integral/proportional derivative controllers based on existence conditions, Proc. Inst. Mech. Eng., Part I, J. Syst. Control Eng. 233 (2018) 384–391.
[41] R. De Keyser, C.I. Muresan, C.-M. Ionescu, An efficient algorithm for low-order direct discrete-time implementation of fractional order transfer functions, ISA Trans. 74 (2018) 229–238.
[42] W. Jifeng, L. Yuankai, Frequency domain analysis and applications for fractional-order control systems, J. Phys. Conf. Ser. 13 (13) (2005) 268–273.